T3.5-P43 SURFACE REFLECTION ARRIVALS FROM SHALLOW SMALL MAGNITUDE EXPLOSIONS USING THE CEPSTRUM TECHNIUQUE—A NUMERICAL ANALYSIS

C. K. Saikia, I. M. Tibuleac, M. Woods, J. Dwyer, and R. C. Kemerait
Air Force Technical Applications Center, Patrick, FL 32925, USA

ABSTRACT: In this paper, we develop a technique based on "pruning of the COMPLEX CEPSTRUM (CC)" for partitioning the waveforms to the up-going (UP, assumed mostly comprising of the surface reflections) and down-going (DN) wavefields. Using synthetic waveforms, we computed CCs and pruned the UP phases to obtain the DN phases. Essentially, we recover the DN wavefield by minimizing the interference of the UP phases. To validate this algorithm, several suites of frequency-wavenumber P-wave seismograms for the UP, DN and total (TT) wavefields were computed for varying depths (<1 Km) and distances (< 400 Km). CCs were computed using a subset of TT wavefields and pruned to compute the UP and DN wavefields assuming the depth as unknown and distance only accurate to within 5 km. The partitioned UP and DN wavefields were compared against the computed F-K UP and DN wavefields. The success was limited as expected. Next, we reanalyzed the waveforms using UP and DN wavefields as templates with known depths and source type, which improved the agreement. At this developmental stage, we attempted to match only the major phases in the partitioned waveforms. We are currently exploring the influence of the elastic and anelastic velocity models that generate the well developed phases. The focus of this paper is to illustrate the approach and its effectiveness. The UP and DN wavefields also provide the delay time of the pP relative to the P onset, and together with ray based travel-time analysis provide help to examine the error in the delay time and relate to the source depth. We examined the accuracy of the delay time of the onsets of UP wavefield relative to DN wavefield by using both real (RC) and complex (CC) cepstra. Results from the RC analysis were more accurate. In future studies, we plan to apply the method to the noise-contaminated data, as well as to data from low-yield shallow events recorded at regional distances. We will also apply ray-based travel times to prune the CCs.

CEPSTRUM – THEORY: In this section, we provide a brief summary on the theory for both RC and CC, and illustrate the potential of CC in constructing the UP and DN wavefields when the wavefield TT is recorded, Let represent TT by a function f(t). The RC of f(t) is the inverse of the logarithm of the power spectrum of the TT wavefield. Phase is dropped and so is not useful in recovering the original time function f(t). It preserves the delay times of various echoes in the function f(t). In the cepstrum analyses, the first echo is the pP wave.

In the case of CC, the phase of the function f(t) is preserved, unwrapped and its trend removed. Therefore, it is possible to recover the original signal f(t) by reversing the process and minimizing phases (Childers and Durling, 1975, CD75).

Given a time series f(t), we equivalently express it as $$f(t)=\int_{-\infty}^{+\infty}F(\omega)e^{i\omega t}d\omega \Longleftrightarrow\Longrightarrow |F(\omega)|e^{i\theta(\omega)}$$

where F(ω) is the Fourier transform of the time function f(t) and is obtained by the Fast-Fourier transformation (FFT).

Its REAL CEPSTRUM (RC) is obtained by the formula $$\Im_{RC}(t)=\int_{-\infty}^{+\infty}\log\left|F(\omega)\,F^{*}(\omega)\right|e^{i\omega t}d\omega$$

Its COMPLEX CEPSTRUM (CC) is obtained by $$\Im_{CC}(t)=\int_{-\infty}^{+\infty}\left[\log|F(\omega)|+j\,\bar{\theta}(\omega)\right]e^{i\omega t}d\omega$$

In CC of the total wavefield, phases belonging to UP wavefield can be pruned (Markel, 1971). In CD75, there is a discussion on techniques for pruning these undesired phases. In this illustration, we used a very simple approach (Tibuleac et al, 2017 SnT meeting, Vienna, oral presentation). We are developing other schemes to improve the pruning because many rays interfere in the P-wave window. The interaction of rays is a complicated and can not easily be deciphered. Note that the phase function in the above expression is unwrapped and trend removed of the original phase θ(ω). The following mathematical approach summarizes the steps used to recover the DN wavefield from the TT wavefield by pruning the UP wavefield.

$$\bar{\Im}_{CC}(t)\Longleftrightarrow\Longrightarrow|\Im_{CC}(\omega)|e^{\bar{\theta}(\omega)}\Longleftrightarrow\Longrightarrow e^{|\Im_{CC}(\omega)|}e^{\bar{\theta}(\omega)}\Longleftrightarrow\Longrightarrow\bar{f}(t)$$

$$\bar{\Im}_{CC}(t) = \text{pruned CC - [UP wavefield minimized]}$$

$$\bar{\theta}(\omega) = \text{phase of pruned CC}$$

$$\bar{f}(t) = \text{DN wavefield}$$

TOTAL WAVEFORM : PARTITION to UP AND DOWN WAVEFIELDS: Figure 1 is a schematic diagram illustrating the proposed technique of partitioning TT wavefield. Left shows a regional P seismogram at 390 Km for an explosion source at a depth of 450m. The crustal model consisted of 7 layers. The middle panel is a display of the agreement between the numerically generated UP and DN seismograms (shown by red traces) and partitioned UP and DN seismograms processed by pruning the CC of the left seismograms. The red traces were computed using a code developed based on the frequency-wavenumber integration technique (Saikia, 1994). Note the partitioned seismograms matched fairly well. The sum of the UP and DN wavefields displayed in the right and compared. Note that the numerical UP and DN wavefields were used as templates while pruning CC to minimize the interference of either UP or DN wavefield.

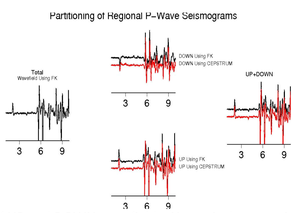

Figure 1. A Schematic display of UP and DOWN wavefields: Numerical vs. pruning of the complex cepstrum (CC).

Figure 2 is a schematic illustration of how the pruning task is accomplished using two cases of seismograms: left: consists of the onset and an echo of opposite polarity at 0.15s with 0.6 times amplitude [pP+P]; middle: with an additional echo at 0.17s with 0.4 times of the onset amplitude with +ve polarity [pP+P+sP]. CC/RC represents comparison of CC (red) and RC (blue). In the middle panel, the first unwanted echo was pruned and in the right panel an additional unwanted echo was pruned to illustrate the effect of pruning progressively from the resulting CCs successively. At this early stage of development of the algorithm, knowing how seismic phases are generated by a velocity model appear useful to develop metrics in this partitioning of wavefields.

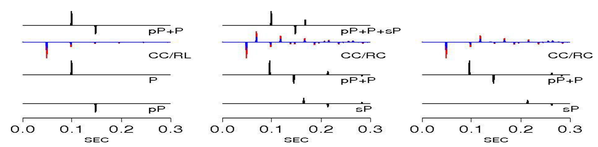

Figure 2. Illustration of progressive "PRUNNING" which we refer to as "reduction of unwanted phases" and often to referred to as "minimization-phase recovery in the CEPSTRUM analysis.

F-K SYNTHETIC WAVEFORM DATA

Using a seven-layered crustal model, we computed a suite of P-wave seismograms for four randomly selected depths at 300m, 450m, 600m, and 750m at receivers with range varying from 50 to 400 km for multiple source mechanisms. The Nyquist frequency was set at 70Hz. Waveforms were decimated to the sampling rates of 100 and 40 samples/second which are often used for recording broadband data in the field. Figure 3 shows P_n & P_n+PmP for both sampling rates at three distances for both elastic and anelastic crustal models, illustrating the relative advantage of the increased sampling rate, if any.

The P- and pP-ray interaction simulated is also observed in seismograms recorded from explosions. This seismic-ray interaction that occurs at various distances is essential to understand for developing constraints to implement waveform partition successfully, because depending upon the number of times an UP-going ray is reflected at the free surface, it can appear in phase in polarity as a DOWN-going ray from the source.

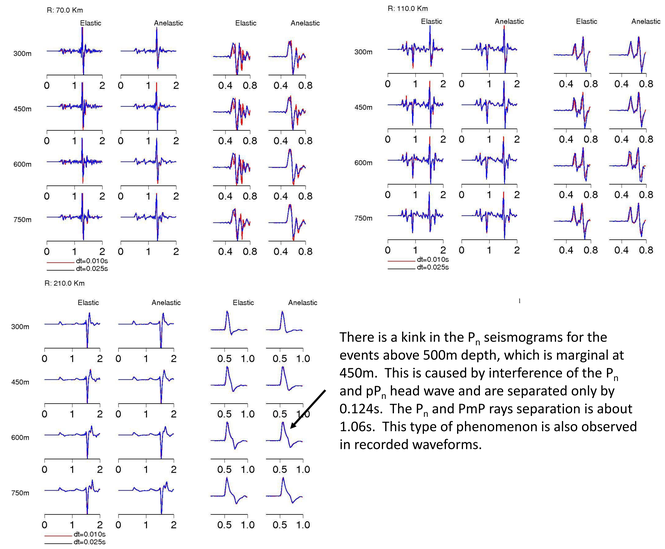

There is a kink in the P_n seismograms for the events above 500m depth, which is marginal at 450m. This is caused by interference of the P_n and pP_n head wave and are separated only by 0.124s. The P_n and PmP rays separation is about 1.06s. This type of phenomenon is also observed in recorded waveforms.

Figure 3. Frequency-wavenumber P-wave seismograms computed using the F-K synthetic code developed by Saikia (1994). We used a phase velocity window so that only the P-waves are trapped in the F-K kernel prior to the application of integration over the wavenumber domain. This helped to reduce the computing time significantly.

PARTITIONING OF WAVEFIELD USING COMPLEX CEPSTRUM

In the following (Figure 4 & 5), we show results of this investigation conducted for the elastic (NQ) and anelastic (Q) models, source types (explosion ZEX vs double-couple ZDS), event depths (300m vs 600m) and distances (50 KM vs 110 KM).

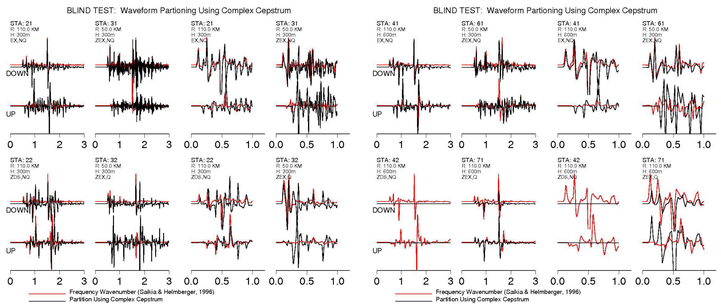

Figure 4. Unwanted phase minimization using the pruning of CC as an illustration of a blind test with no depth information. Distances were available up to an error of ±5 KM. Agreement in the partitioned waveforms for some prominent phases is marginal.

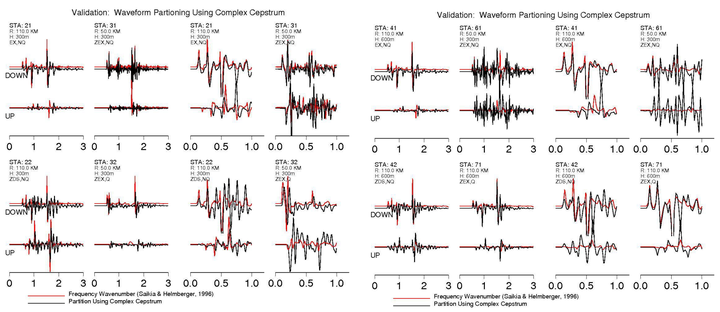

Figure 5.Reprocessing of the same waveforms with the known depths and distances, including the UP and DOWN wavefields available as templates. This analysis shows an improved agreement between the partitioned and the numerical UP and DOWN wavefields.

The waveform fits can be improved by advanced "pruning" strategies of the unwanted/minimization of the phase interference. To do this, a library of path-specific UP and DOWN seismograms as a function of depths will be created and partitioning will be done for the TT wavefield.

1st ECHO DELAY TIME – RC vs. CC

The delay time of the 1st echo is related to the depth, which is estimated by assuming that the delay time equals the two-way travel time for the P wave from the source to the surface. Any error in the delay time and the P-wave velocity in the source structure lead to error in this depth estimate. Delay times are often affected by factors: (i) the poor signal-to-noise ratio and (ii) the complexity in the geology and topography models. The CEPSTRUM analysis is aimed at estimating this delay time, but is indeed difficult for shallow events.

To overcome the shallow depth problem, one proposal is to record signals with a sampling rate higher than the 40 samples/second (often used in broadband field operation). Synthetic results presented in Figure 4 does not support this hypothesis. For stations at large distances, the Q effect is strong , which makes the details in the pP + P interaction disappear by about 100 Km. On the other hand, this is the primary feature that the CEPSTRUM method tries to focus on. In Figures 6 &7, we summarize results of CEPSTRUM analysis using the F-K seismograms. We find that the 1st echo delay time estimated using the RC analysis is better than the delay time estimated using the CC analysis.

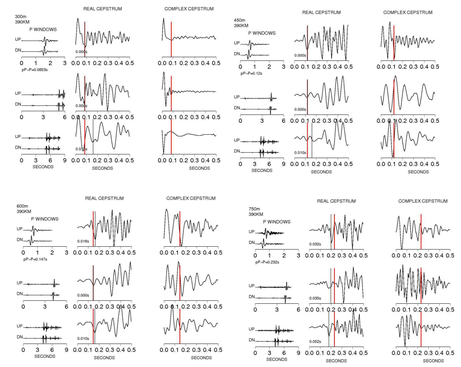

Figure 6. Vertical lines correspond to delay time of the 1st echo relative to the onset: red predicted from the crustal model and dark based on the RC and CC analysis. Left column shows the signal widow used in the analysis. Small window length and the RC analysis produced the best results. The CC analysis was very sensitive to oscillations in the traces and was controlled by the filtering the CCs. The delay time appeared sensitive to the filter parameters, which is problematic because one may not have any prior information on the model.

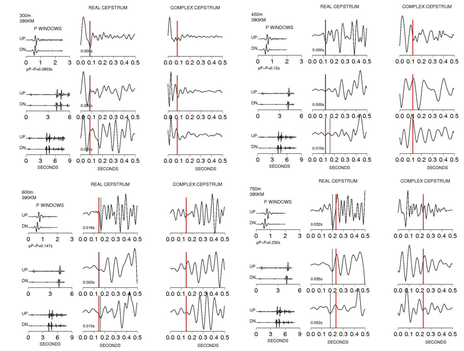

Figure 7. Examples for the anelastic case. It is obvious that RC provides a better estimate of the delay time. "Pruned CC" and RCs were filtered between 4 and 45 Hz after applying a tapering window. Each trace has undergone the same post processing.

CONCLUSIONS

- **REAL CEPSTRUM (CC) analysis predicts arrival times of the 1st ECHO more accurately than the CC analysis.**
- **Presence of NOISE deteriorates the details of the pP and P head-wave interaction**. To overcome this problem, we are extending this method to PmP (geometrical) rays; these rays remain above the noise level. DE-NOISING will be applied.
- TT wavefields can be partitioned to its UP and DOWN wavefields using the PRUNING of CC.
- **Delay time of the UP wavefield onset relative to the DN wavefield onset is the delay time of the 1st ECHO.**
- **Delay time Δt of the 1st ECHO can be used to estimate the DOB by using:**

$$\Delta t_{1st\,Echo}=2.\sum_{j=1}^{n}th_j\eta_j \qquad \text{where } \eta_j \text{ is the vertical slowness; } th_j \text{ is the thickness of the layer}$$

- To recover the DOWN wavefield, the UP wavefield contributions are pruned out of the CC, and vice versa. **The numerical templates of the UP and DOWN wavefields provide the guidelines to accomplish this goal and develop new metrics.**
- **Both UP and DOWN wave field's rays may remain in phase**, which makes the application of the PRUNING of CC difficult. Research is continuing to address this issue.
- **Regional P seismograms computed for both 40 samples and 100 samples/second do not exhibit discernable waveform characteristics, especially for the anelastic model**. The Qp values were set at 60 in the top 1 Km, 100 in the next 1 Km, and for the remaining of the deeper layers was at 500. These are not even the extreme Q values for a velocity model.

REFERENCES:
Childers and Durling (1975) Digital Filtering and Signal Processing, West Publishing Company, ISBN 0-8299-0056-X
Saikia, C. K. (1994).. Modified frequency-wavenumber algorithm for regional seismograms using Filon's quadrature: modeling of Lg waves in eastern North America, DOI: 10.1111/j.13650246X.1994.tb04680.X, Vol, 118, 142-158.
Saikia, C. K. and D. V. Helmberger (1997) . Approximation of Rupture Directivity in Regional Phases Using Up-going and Down-going Wave Fields, Bull. Seis. Soc, Am. 87, 097-998.
ACKNOWLEDGEMNTS: We thank Dr. M. THUSRBY for developing the matlab code which was used in "pruning" of CC